The Astrophysical Journal, 661:1297–1310, 2007 June 1

BULK FLOW VELOCITY AND FIRST-ORDER ANISOTROPY OF SOLAR ENERGETIC PARTICLES OBSERVED ON THE *WIND* SPACECRAFT: OVERVIEW OF THREE "GRADUAL" PARTICLE EVENTS

Lun C. Tan,[1] Donald V. Reames, and Chee K. Ng[2]
NASA Goddard Space Flight Center, Greenbelt, MD 20771; ltan@mail630.gsfc.nasa.gov
Received 2006 November 20; accepted 2007 February 17

ABSTRACT

We have developed techniques to calculate bulk flow velocity and first-order anisotropy of solar energetic particles (SEPs) with MeV nucleon^{-1} energies as recorded on the *Wind* spacecraft. Using the techniques we selected and analyzed three gradual SEP events having different solar longitudes. Since upstream of interplanetary (IP) shocks during our selected events the interplanetary magnetic field is nearly perpendicular to the solar wind, the diffusive transport of SEPs along the magnetic field line is conveniently decoupled from solar-wind streaming. We present the bulk flow velocity measurements of H, He, O, and Fe ions at different energies. In two of the three events studied, it is seen that the flow directions of heavy ions reverse in sequence, i.e., faster ions reverse their direction earlier. Several hours before the IP shock passage, the bulk flows of all heavy ions become opposite to the proton flow. Thus, in the upstream region we mainly observe shock-accelerated protons that continue to flow away from the shock, while higher rigidity heavy ions predominantly come from strong acceleration near the Sun. The reversed ion direction appears also to involve a reflecting boundary beyond 1 AU, from which higher velocity ions return earlier. The preferred geometry of the selected 2001 September 24 event also allows us to determine the propagating direction of proton-generated Alfvén waves based on flow velocity measurements of heavy ions.

Subject headings: acceleration of particles — interplanetary medium — shock waves — Sun: coronal mass ejections (CMEs) — Sun: particle emission

1. INTRODUCTION

Evidence gathered in recent years indicates the presence of two kinds of distinctive solar energetic particle (SEP) events (Reames 1999 and references therein): large "gradual" SEP events, in which particles are accelerated at shock waves driven by fast coronal mass ejections (CMEs) from the Sun, and small "impulsive" SEP events, in which particles are originated from resonant wave particle interactions in the flare plasma. Since large gradual SEP events create a hazardous environment for space exploration systems, the acceleration and transport of SEPs during these events remain a focus of the National Space Weather Program and NASA Living with a Star Program and an outstanding question in solar-terrestrial physics.

Being different from composition or energy spectrum measurement, the anisotropy analysis of SEPs can provide information on particle distributions in space. In fact, among measurements using a single spacecraft, the composition or energy spectrum observation only presents a "point" analysis in space, while the anisotropy analysis may be used to infer the spatial distribution of SEPs in two or three dimensions. In addition, the evolution of composition or energy spectrum of SEPs often contains a cumulative effect of particle transport through spatially and temporally varying wave fields from the Sun to the spacecraft. In contrast, the anisotropy analysis is a more direct display of particle distributions in the local environment (e.g., Reames & Ng 2002).

There is a significant difference of ion anisotropies between the gradual and impulsive SEP events. In the gradual event, after an initial increase, the anisotropy is usually small and first order in nature (Dwyer et al. 1997; Reames et al. 2001). In contrast, in the impulsive events the anisotropy is large and "exponential" in nature (Mason et al. 1989). Since in this work we are concerned with the gradual SEP event, we only examine the first-order anisotropy of SEPs.

Earlier works on the anisotropy analysis were intended to explain the variation of proton anisotropies during different phases of SEP transport processes (e.g., McCracken & Ness 1966; McCracken et al. 1971; Forman 1968; Ng & Gleeson 1971). Later, during the *International Sun-Earth Explorer 3* (*ISEE 3*) era the analysis was also used to examine protons and α-particles in the upstream (Sanderson et al. 1985; Tan et al. 1989) and downstream (Tan et al. 1988) regions of IP shocks. Recently, new observations on SEP anisotropies have been carried out on the *Advanced Composition Explorer* (*ACE*; Lesky et al. 2001), *Ulysses* (Zhang et al. 2003; Sanderson et al. 2003), and *Wind* (Dwyer et al. 1997; Reames et al. 2001; Reames & Ng 2002) spacecraft and on ground-level experiments (e.g., Bieber et al. 2002). In particular, Reames et al. (2001) measured the angular distributions of H, He, O, and Fe ions in MeV nucleon^{-1} range under a variety of conditions. They noted that SEP streams are organized by plasma β-values. Nevertheless, the front/back ion intensity ratio introduced by them to represent the first-order anisotropy of ions may face some difficulties when comparison is made with theories. It is necessary to develop techniques that can exactly calculate the theoretical anisotropy given in Ng & Wong (1979) and Gleeson & Webb (1980).

At lower energies ($\sim$0.1 MeV nucleon^{-1}; see, e.g., Tan et al. 1988, 1992a; Dwyer et al. 1997) the calculation of ion first-order anisotropy in the solar-wind frame is not trivial because of the complexity in the transformation that converts the ion angular distribution from the spacecraft frame to the solar-wind frame (Ipavich 1974; Sanderson et al. 1985; Ng 1986). The complexity results from the ion velocity being comparable to the solar-wind speed. By introducing the concept of the rest frame, in which the

[1] Also at Perot Systems, Fairfax, VA 22031.
[2] Also at Department of Astronomy, University of Maryland, College Park, MD 20742.

phase-space distribution function of ions is assumed to be isotropic, Gloeckler et al. (1984) simplified the calculation of ion first-order anisotropy. They noted that the velocity of the rest frame relative to the spacecraft frame is the bulk flow velocity of ions, which is related to the ion first-order anisotropy in the solar-wind frame through simple vector relationships (Forman 1970; Tan et al. 1992a). Nevertheless, iteration calculations are still necessary in order to estimate the bulk flow velocity of ions (Tan et al. 1988, 1992a). In addition, it should be emphasized that these vector relationships are valid only if the transverse spatial gradient anisotropy of ions is negligible relative to their diffusive anisotropy.

However, in the MeV nucleon^{-1} energy range available to the *ACE* and *Wind* spacecraft, the difficulty in the calculation of ion bulk flow velocities would no longer exist, because the ratio of the solar-wind speed to the ion speed is much less than unity ($\sim$0.01). Thus, in the expansion of ion phase-space distribution functions, only the first-order terms need to be kept, leading to a straightforward calculation of ion bulk flow velocities. The flow analysis technique thus developed should be suitable for examining the gradual SEP events, in which ion anisotropies are mainly first order in nature, as observed by the Low-Energy Matrix Telescope (LEMT) of the Energetic Particles: Acceleration, Composition, and Transport (EPACT) experiment on *Wind* (von Rosenvinge et al. 1995). The LEMT sensor, by supplying the count rate data of H, He, O, and Fe ions in 16 sectors relative to the local magnetic field direction, so far has provided the best resolution of ion angular distributions in the MeV nucleon^{-1} energy range (see Reames et al. 2001).

Three gradual SEP events with different solar longitudes have been selected for our analysis. Since upstream of IP shocks the selected events have the interplanetary magnetic field (IMF) direction nearly perpendicular to the solar wind, the local diffusive transport of ions along the magnetic field line can be conveniently decoupled from solar-wind streaming. Consequently, effects of ion scattering centers can be clearly displayed.

In order to provide an overview of bulk flow velocity and first-order anisotropy of SEPs in this paper, we examine the angular distributions of H, He, O, and Fe ions at different energies during different evolving phases in our selected events. The organization of the paper is as follows. First, we introduce techniques used to calculate the bulk flow velocity and first-order anisotropy of ions. Then, we present ion bulk flow velocity observations during different phases in our selected events. In particular, we examine differences of bulk flow directions between protons and heavy ions and identify possible reasons that cause the differences. In addition, by using the bulk flow velocity data of heavy ions, we determine the propagating direction of Alfvén waves mainly generated by proton streaming.

2. EXPERIMENTAL METHOD

2.1. *Observed Data*

As described above, we analyze the sectored count rate data of different ion species and energies obtained by the LEMT sensor on the *Wind* spacecraft, which spins with a 3 s period around an axis perpendicular to the ecliptic plane (von Rosenvinge et al. 1995). The LEMT sensor is a domed array of 16 silicon detectors with a total geometric factor of 51 cm^2 sr. On the ecliptic plane the ion angular distribution data given in 16 sectors are measured with respect to the local magnetic field direction with a time resolution of 1 hr (see Reames et al. 2001 for details). In addition, the LEMT sensor provides the energy spectral data of heavy ions, although the proton energy spectral data are obtained from the *Interplanetary Monitoring Platform 8* (*IMP 8*) 30 minute intensity data set archived in the NASA CDAWeb.[3] The magnetic field and solar-wind data used in the analysis are obtained from the observations of the Magnetic Field Experiment (MFE) and Solar Wind Experiment (SWE) on the *Wind* spacecraft; data from these two are also archived in the NASA CDAWeb with a time resolution of $\sim$1 minute.

2.2. *Definition of Bulk Flow Velocity Vector of Ions*

The theoretical first-order anisotropy $\boldsymbol{A}_1$ of ions described above is a vector, whose projection along a direction $\boldsymbol{a}$ in the spacecraft frame is

$$(\boldsymbol{A}_1)_{\boldsymbol{a}} = 3 \int \mu f(\mu)\, d\Omega \Big/ \int f(\mu)\, d\Omega, \qquad (1)$$

where the integral is over all solid angles (Ω), f is the phase-space distribution function of ions, and μ is the cosine of the angle between $\boldsymbol{A}_1$ and $\boldsymbol{a}$.

Here, $\boldsymbol{A}_1$ is calculated by solving for the velocity $\boldsymbol{V}_F$ of the "rest" frame, in which the first-order anisotropy of f vanishes. The velocity $\boldsymbol{V}_F$ is also the ion bulk flow velocity relative to the spacecraft frame. Our definition is an extension of that previously used by Gloeckler et al. (1984), who assumed that f is isotropic in the rest frame. In our generalized definition, the rest frame would always exist.

Nevertheless, the conceptual usefulness of the rest frame depends on the status of ion streams examined. In the absence of waves, ion velocity will have a beamlike "exponential" distribution (Roelof 1969; Gordon et al. 1999), as observed, e.g., in the early phase of an impulsive SEP event. Although the rest frame exists with large $\boldsymbol{V}_F$, they are not useful, as they do not reflect a quasi-equilibrium. On the contrary, in the presence of waves, a quasi-equilibrium state of ion streams can be established with a broadened pitch-angle distribution and small anisotropy of ions. As the second and higher order anisotropies are diminished, the resultant anisotropy of ions will be first order in nature as observed in the gradual SEP event. Consequently, the rest frame concept is useful in describing the streaming of ions.

Therefore, the key factor to assure the conceptual usefulness of the rest frame is that the first-order anisotropy is $<$0.5, and higher order anisotropies are even smaller. In order to quantify the applicable range of our technique, it is adequate to show that the second- and third-order anisotropies are indeed small. In Figure 1 the relative magnitudes of anisotropies at different orders as projected to the local magnetic field direction are shown for the 1998 September 30 event. It is clear that except for (1) the first 4 hr after the occurrence of the relevant W85° flare and (2) the Fe (2.5–5 MeV nucleon^{-1}) ion data after day $\sim$1.5 of 2000 October (because of poor statistics of Fe data), the relative magnitude of the second- and third-order anisotropies of all ions are indeed small, justifying our calculation of $\boldsymbol{V}_F$. Hence, we expect that the technique is applicable to the entire upstream region (except for the first few hours during the onset phase) of gradual SEP events.

2.3. *Relation between Bulk Flow Velocity and First-Order Anisotropy of Ions*

Forman & Gleeson (1975) derived the total anisotropy of ions as the sum of both diffusive and convective components. The convective component is caused by solar-wind streaming due to

[3] See Web site at http://cdaweb.gsfc.nasa.gov.

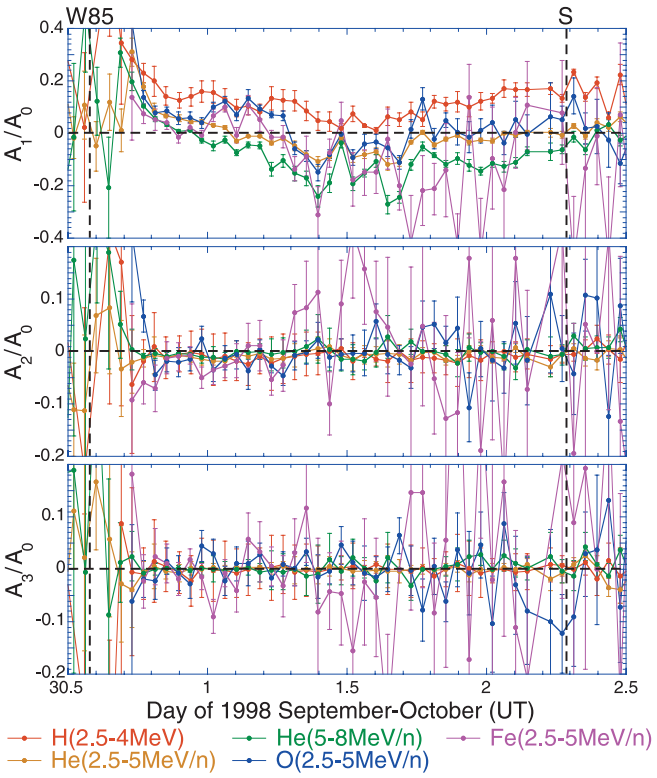

FIG. 1.—Time profiles of relative magnitudes of ion anisotropies at different orders as projected to the local magnetic field direction for the 1998 September 30 SEP event. Note that the scale of ordinates among different panels is different.

the Compton-Getting effect (Gleeson & Axford 1967). Thus, Forman (1970) estimated the ion anisotropy introduced by the motion of an observer with the velocity $-\boldsymbol{V}$ relative to the ion flux. Based on the Lorentz invariance of ion phase-space distribution functions, for nonrelativistic ions to the order of V/v, an additional Compton-Getting anisotropy

$$\boldsymbol{A}_{1\mathrm{CG}} = -[d \ln F_0(v)/d \ln v](\boldsymbol{V}/v), \tag{2}$$

where $F_0(v)$ is the omnidirectional phase-space distribution function of ions and the $-[d \ln F_0(v)/d \ln v] \cong \gamma$ index in The Power-law approximation should be added to the anisotropy of ions (also see Tan et al. 1992a). Since the rest frame has the velocity $\boldsymbol{V}_F$ in the spacecraft frame, the rest frame should have the velocity $\boldsymbol{V}_F - \boldsymbol{V}_{\mathrm{SW}}$ ($\boldsymbol{V}_{\mathrm{SW}}$ being the solar-wind velocity) in the solar-wind frame. Therefore, the spacecraft frame and the solar-wind frame should have $-\boldsymbol{V}_F$ and $-(\boldsymbol{V}_F - \boldsymbol{V}_{\mathrm{SW}})$ in the rest frame, respectively. Since the first-order anisotropy of ions in the rest frame is zero, according to equation (2) the observed anisotropy should be

$$\boldsymbol{A}_1 = \gamma \boldsymbol{V}_F/v \tag{3}$$

and

$$\boldsymbol{A}_{1s} = \gamma(\boldsymbol{V}_F - \boldsymbol{V}_{\mathrm{SW}})/v, \tag{4}$$

in the spacecraft frame and solar-wind frame, respectively. Equation (3) shows the direction of the ion first-order anisotropy in the spacecraft frame ($\boldsymbol{A}_1$) being the same as $\boldsymbol{V}_F$. In addition, equation (4) indicates that the ion first-order anisotropy in the solar-wind frame ($\boldsymbol{A}_{1s}$) can be deduced from $\boldsymbol{V}_F$ through simple vector computations.

2.4. *Deduction of Bulk Flow Velocity of Ions*

Since the LEMT data that we analyze are projected onto the spin plane, a two-dimensional (radius r and azimuthal angle ϕ) approximation is suitable for the deduction of $\boldsymbol{V}_F$. Here we first search for the azimuthal angle ϕ_F of $\boldsymbol{V}_F$. It is obvious that $(\boldsymbol{A}_1)_{\boldsymbol{a}}$ should be at maximum if $\boldsymbol{a}$ coincides with $\boldsymbol{A}_1$. Therefore, by setting $d(\boldsymbol{A}_1)_{\boldsymbol{a}}/d\phi_F = 0$ from equation (1), where $\mu = \cos(\phi - \phi_F)$, we have

$$\sum_{i=1}^{N} \sin(\phi_i - \phi_F) C_i = 0, \tag{5}$$

where C_i is the count rate of ions in the sector i of the LEMT sensor having $N = 16$ sectors. Solving equation (5) numerically, we obtain ϕ_F.

We then calculate the magnitude of $\boldsymbol{V}_F$. Owing to the invariance of ion phase-space distribution functions (Forman 1970) that $f(\boldsymbol{v}) = f^*(\boldsymbol{v}^*)$, where the asterisk denotes the rest frame (in contrast, no superscript is added to the quantity in the spacecraft frame), and taking the "local" power-law approximation assuming $f^*(\boldsymbol{v}^*) \propto (\boldsymbol{v}^*)^{-\gamma^*}$ being applicable to each energy bin of ions, we obtain

$$f(\boldsymbol{v}) \propto (\boldsymbol{v}^*)^{-\gamma^*}, \tag{6}$$

where γ^* is the power-law index of f^*. Since $\boldsymbol{v}^* = \boldsymbol{v} - \boldsymbol{V}_F$, we further have

$$KC_i = |\boldsymbol{v}_i - \boldsymbol{V}_F|^{-\gamma^*}, \tag{7}$$

where K is a constant and $\boldsymbol{v}_i$ is the ion velocity vector in sector i. Because of the assumption that $V_F/v \ll 1$, by expanding equation (7) to the first order of V_F/v, we obtain

$$v[1 - (2V_F/v)\cos(\phi_i - \phi_F)]^{1/2} = (KC_i)^{-1/\gamma^*}. \tag{8}$$

Since $\gamma^* = \gamma$ at $V_F/v \ll 1$ (Ipavich 1974), equation (8) is further simplified to

$$\ln(C_i)/\gamma = A - (V_F/v)\cos(\phi_i - \phi_F), \tag{9}$$

where A is a constant, and

$$\gamma = 2(\gamma_0 + 1), \tag{10}$$

where γ_0 is the spectral index of ion differential intensity with respect to ion kinetic energy (Ipavich 1974).

Therefore, by plotting $\ln(C_i)/\gamma$ against $\cos(\phi_i - \phi_F)$, we can calculate the V_F/v (and hence V_F) value from the slope of fitted straight lines. In Figure 2 the energy spectra data of H, He, O, and Fe ions with their polynomial fits are shown for a 5 hr interval in the 1998 September 30 event. In addition, for a 1 hr period given at the center of the 5 hr interval shown in Figure 2, plots of $\ln(C_i)/\gamma$ against $\cos(\phi_i - \phi_F)$ (see eq. [9]) are displayed in Figure 3, where the γ value in each energy bin of ions is estimated at the ion mean energy. Thus, from Figure 3 the following points can be summarized.

1. For each ion species the observed data are very well fitted by a straight-line relationship, indicating that the anisotropy of ions during the examined period is indeed first order in nature.
2. The deduced V_F value has a high accuracy. In particular, for He ions the absolute error of estimated V_F values is ± 10 km s^{-1},

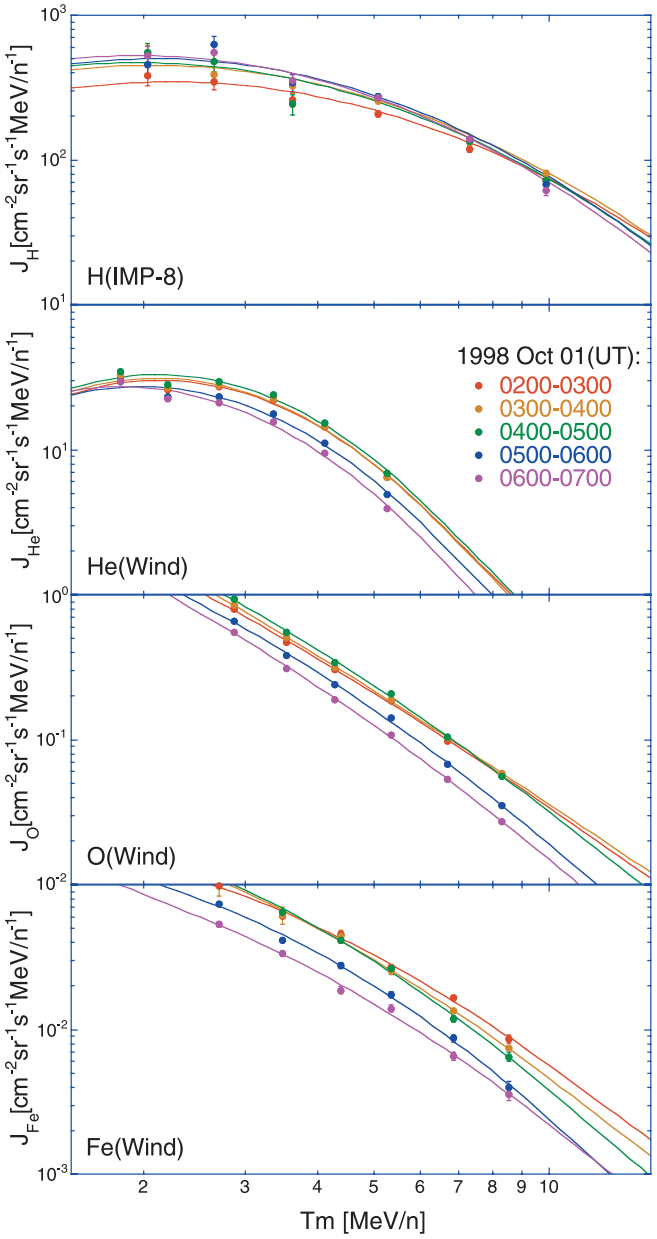

FIG. 2.—During the 1998 September 30 SEP event energy spectra of different ion species are shown for a 5 hr interval denoted by the shaded pink region in Fig. 4.

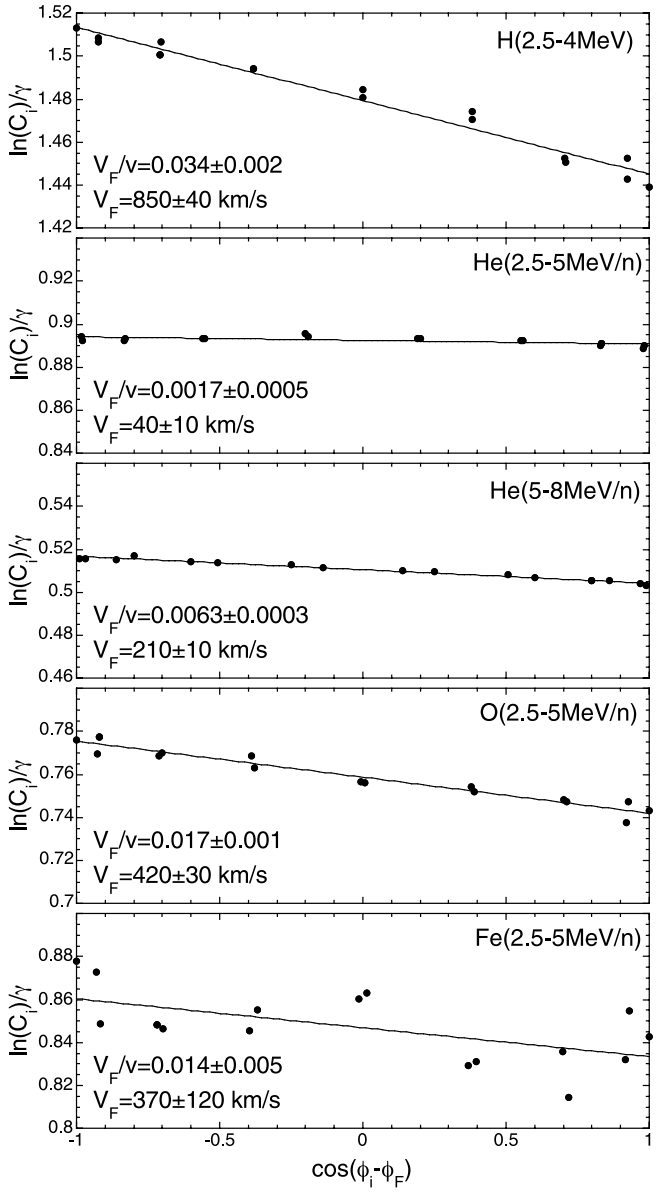

FIG. 3.—During a 1 hr period located in the center of time interval sampled in Fig. 2 plots of ln $(C_i)/\gamma$ against cos $(\phi_i - \phi_F)$ are shown for different ion species.

which is less than the Alfvén speed V_A, making it possible to examine the propagating effect of Alfvén waves.

3. OBSERVATIONS

3.1. *Criteria of Event Selection*

For gradual SEP events we examine the entire time interval between the onset and the arrival of the IP shock, consisting of the onset, "plateau," and the energetic storm particle (ESP) enhancement phases according to the classification of Lee (2005). We will leave the downstream region after IP shock passage for future examinations. In order to present an overview of the bulk flow velocity and first-order anisotropy of different ion species, we show time profiles of ion bulk flow characteristics in typical gradual SEP events having significantly different solar longitudes of associated flares and CMEs.

Since the bulk flow velocity measurement of ions was used to examine the ESP enhancement at proton energies of ~0.1 MeV (Tan et al. 1989), we need to clarify a fundamental difference of ion scattering characteristics between ESPs at ~0.1 MeV nucleon^{-1} examined there and SEPs at ~4 MeV nucleon^{-1} concerned here. Taking the famous 1978 November 12 ESP event as an example, the deduced scattering mean free path of ~0.1 MeV protons is $\lambda \sim 5 \times 10^{-4}$ AU (see Table 2 in Tan et al. 1989), and the scale length of the upstream region is $l \sim 4 \times 10^{-3}$ AU. Hence, we have $l/\lambda \sim 8$, indicating that ESP ions experience many chances of scattering before escaping from the upstream region. On the contrary, from the simulations of Ng et al. (2003) we find that $\lambda \geq 0.2$ AU for He ions of ~4 MeV nucleon^{-1} in the plateau region (see Fig. 3 in Ng et al. 2003). Suppose that the duration of the plateau region observed by the *Wind* spacecraft is ~1 day, with an averaged $V_{SW} \sim 400$ km s^{-1}, we obtain the scale length of the plateau region $l \sim 0.2$ AU. We therefore have $l/\lambda \leq 1$, indicating that SEPs experience fewer scatterings inside the plateau region.

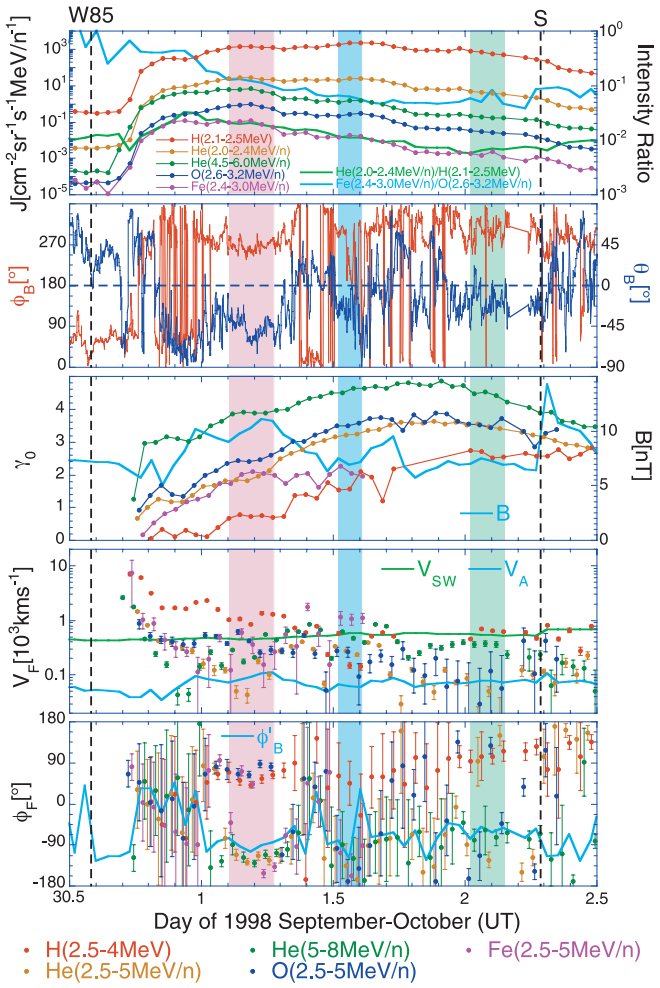

FIG. 4.—Time profiles of the ion intensity (J), intensity ratio, azimuth (ϕ_B), latitude (θ_B), and magnitude (B) of IMF, ion energy spectral index (γ_0), solar-wind speed (V_{SW}), Alfvén speed (V_A), ion bulk flow speed (V_F), and azimuthal angle (ϕ_F) of different ion species during the 1998 September 30 SEP event.

Because V_{SW} usually dominates V_A by an order of magnitude, when we select SEP events that have $\boldsymbol{B}$ nearly perpendicular to $\boldsymbol{V}_{SW}$ in the upstream region, the component of $\boldsymbol{V}_{SW}$ along $\boldsymbol{B}$ may become comparable to V_A. Hence, by observing the ion anisotropies, it is possible to detect the propagation direction of parallel Alfvén waves, assuming they are responsible for scattering the SEPs.

3.2. *1998 September 30 Event*

This western (W85°) solar longitude event was widely examined by Lario et al. (2000a, 2000b), Reames (2000a, 2000b), Reames et al. (2001), and Tylka et al. (2005). In Figure 4 we use "W85" and "S" to denote the locations of solar flare and IP shock associated with this event, respectively.

Ion intensities are shown in the top panel of Figure 4. This is a large SEP event with peak proton intensity at 2.1–2.5 MeV of $>10^3$ (cm^{-2} sr^{-1} s^{-1} MeV^{-1}), to which the contribution of the IP shock at 1 AU is insignificant. During the onset phase, we observe a rising He/H ratio and descending Fe/O ratio, both of which are due to preferential scattering of lighter ions at earlier time in the event (Reames 2000a; Ng et al. 2003).

Furthermore, energy spectral indices of ion differential intensities are shown in the third panel of Figure 3. The event had a hard proton spectrum, as γ_0 of protons was small in the upstream region. The hard proton spectrum assumption is also supported by Reames et al. (2001), who reported an unusually high intensity of 19–22 MeV protons for the event. In contrast, among the three events examined in this work, the event had the softest energy spectrum of heavy ions as seen from the γ_0 plot in Figure 3.

Finally, bulk flow speeds and flow directions of ions are shown in the fourth and bottom panels of Figure 4, respectively. Since the ion angular distribution measured by the LEMT sensor is defined relative to the local magnetic field direction, we present the IMF azimuthal and latitudinal angles (ϕ_B and θ_B, respectively) in the second panel of Figure 4. It can be seen that during some time intervals (e.g., 1998 September 30, 16:00–24:00 UT) the observed ϕ_B presents significant fluctuations, leading to a large uncertainty in the hourly averaged ϕ_B value, which can propagate into the calculation error of flow direction as shown in the ϕ_F plot. In addition, since the LEMT sensor primarily measures two-dimensional angular distribution of ions, we avoid the use of observed data at $\theta_B > 60^\circ$, as done in Dwyer et al. (1997).

During the onset phase of this SEP event V_F of both protons and heavy ions were large and rapidly declined. In spite of large uncertainties of ϕ_F, the flow directions of all ions were apparently toward the Sun. Sunward flow direction is not rare in our observations and may be caused by a variety of reasons (e.g., due to variable solar wind [see Ng 1987] or looped field lines [see Richardson & Cane 1996]). It should be noted that the blue line in the bottom panel of Figure 4 denotes the "rectified" ϕ'_B that is equal to ϕ_B or $\pi - \phi_B$, depending on which satisfies the ($\leq\pi/4$ or $>5\pi/4$) condition. Therefore, when ϕ_F is equal to ϕ'_B the direction of $\boldsymbol{V}_F$ may be parallel or antiparallel to the real $\boldsymbol{B}$.

It is seen from Figure 4 that after 1998 October 01, 00:00 UT when the *Wind* spacecraft entered into the plateau region, along the magnetic field line higher speed He (5–8 MeV nucleon^{-1}) ions first reversed their flow direction. Then during the interval denoted by the shaded pink region other heavy ions also reversed their flow directions. When the shaded blue region was reached, all heavy ions became opposite to protons. Then both protons and heavy ions kept their flow directions (see the shaded green region) until the shock arrived.

In order to demonstrate the flow reversal of heavy ions, pie plots of ion angular distributions given in the three shaded regions in Figure 4 are shown in Figure 5, where arrows are used to denote the vector averaged over the sampled multihour interval (which becomes more significant when averaged). The following points can be summarized from Figure 5.

1. The ion anisotropy is first order in nature. There is no observation of bidirectional fluxes (e.g., Richardson & Cane 1996) or skew distributions (e.g., only Sun-side sectors having significant counts) of ions, which justifies our deduction procedures of $\boldsymbol{V}_F$.
2. In most cases $\boldsymbol{V}_F$ of different heavy ion species at the same energies are along nearly the same directions, which are opposite to $\boldsymbol{V}_F$ of protons. The exceptional case, however, is seen in the left panels of Figure 5, where the flow reversal of He (2.5–5 MeV nucleon^{-1}) ions is earlier than that of O (2.5–5 MeV nucleon^{-1}) ions.
3. The $\boldsymbol{V}_F$ vector of all ion species is nearly parallel to $\boldsymbol{B}$, and $\boldsymbol{B}$ is nearly perpendicular to $\boldsymbol{V}_{SW}$. Since we have clear evidence showing that protons flow away from the shock (see § 4.3 below), heavy ions should mostly flow toward the weakened shock after reversing their flow directions.

3.3. *2001 September 24 Event*

This eastern (E23°) solar longitude event was listed in Gopalswamy et al. (2004), Kahler (2005), and Tylka et al. (2005).

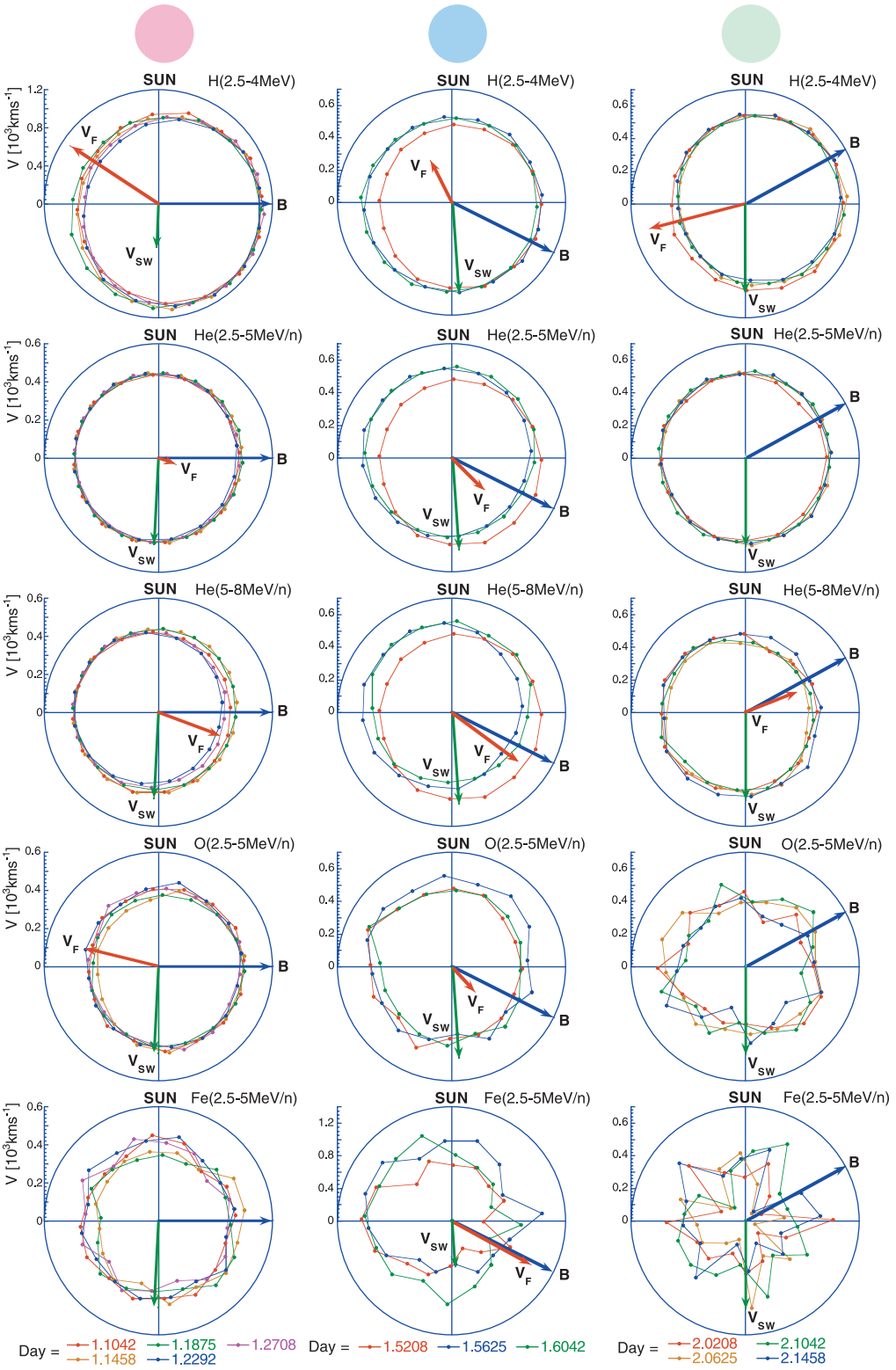

FIG. 5.—Angular distributions of different ion species are shown for three shaded regions given in the preceding figure for the 1998 September 30 SEP event.

In addition, Sanderson et al. (2003) examined this event at ~2 AU and in the solar latitude range of N70°–N80° by using *Ulysses* observations.

Ion intensities during the event are shown in the top panel of Figure 6. This is a large SEP event with the peak proton (2.1–2.5 MeV) intensity of $>10^3$ (cm^{-2} sr^{-1} s^{-1} MeV^{-1}). Being different from the 1998 September 30 event described above, however, there were significant enhancements of ion intensities when the IP shock was crossed. The enhancement of He (2.5–5 MeV nucleon^{-1}) ion intensities was greater than that of proton intensities. There was also no significant change of He/H or Fe/O ion ratio in the upstream region.

Energy spectral indices of ion differential intensities are shown in the third panel of Figure 6. During the event all nearly same

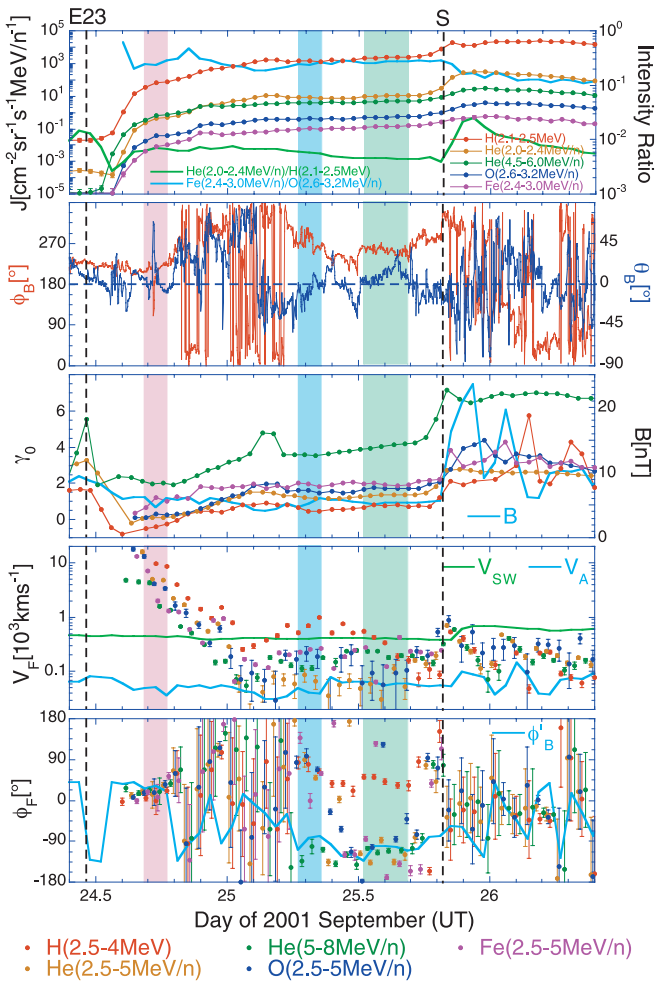

FIG. 6.—Same as Fig. 4, but for the 2001 September 24 SEP event.

speed ion species at 2–5 MeV nucleon^{-1} had small γ_0 values (between 1 and 2), indicating that both protons and heavy ions had hard energy spectra.

Bulk flow speeds and flow directions of ions are shown in the fourth and bottom panels of Figure 6, respectively. Being similar to the 1998 September 30 event described above, during the later rising phase of the event as denoted by the shaded pink region in Figure 6, flow directions of all ion species were apparently toward the Sun. Flow speeds of all ion species were also large and rapidly decreased.

During the plateau phase V_F of heavy ions was less than V_{SW}, but still higher than V_A. Similar to the 1998 September 30 event, the flow directions of heavy ions also reversed in sequence. First, near the shaded blue region the higher speed He (5–8 MeV nucleon^{-1}) ions reversed their flow direction. Then lower speed He, O, and Fe ions (2.5–5 MeV nucleon^{-1}) reversed their flow directions before entering the shaded green region. Finally, along $\boldsymbol{B}$ both protons and heavy ions had flow directions opposite to each other.

For the 2001 September 24 event, pie plots of ion angular distributions are shown in Figure 7. During the later rising phase (*left panels*) $\boldsymbol{B}$ was nearly parallel to $\boldsymbol{V}_{SW}$, and flows of all ions were apparently toward the Sun. It is noted (e.g., Richardson et al. 1991; Richardson & Cane 1996) that the flow direction of SEPs may be significantly different from the Parker spiral field line, especially for the eastern solar longitude event. Furthermore, when the IP shock was approached $\boldsymbol{B}$ became nearly perpendicular to $\boldsymbol{V}_{SW}$, and $\boldsymbol{V}_F$ was nearly parallel or antiparallel to $\boldsymbol{B}$ (*middle and right panels*).

3.4. *1998 November 14 SEP Event*

This western (W120°) solar longitude event was only listed in Tylka et al. (2005). Ion intensities during the event are shown in the top panel of Figure 8. This is a medium-sized SEP event with the peak proton (2.1–2.5 MeV) intensity of $\leq 10^2$ (cm^{-2} sr^{-1} s^{-1} MeV^{-1}). Because of its far western solar longitude origin, no IP shock associated with this event was identified at 1 AU. This point is significantly different from the shock-associated events described above. In addition, in contrast with the smooth variation of He/H ion ratio, the Fe/O ion ratio showed fluctuations during the onset phase of the event.

Energy spectral indices of ion differential intensities are shown in the third panel of Figure 8. In spite of the medium-sized feature of the event, the hard spectra of all ions can be seen from their spectral indices $\gamma_0 = 1$–2 in Figure 8.

Bulk flow speeds and flow directions of ions are shown in the fourth and bottom panels of Figure 8, respectively. Similar to that which we have done for the shock-associated events described above, here we also examine the event during a ~2 day interval starting from the occurrence of the associated flare/CME. On the first day we observe two maxima of ion intensities as denoted by the shaded pink and blue regions in Figure 8. We also observe a dip of V_F between the two maxima, and significant decrease of Fe/O ion ratio before the first maximum. Since the decline of both V_F and Fe/O ion ratio may be observed during the onset phase (see Fig. 4), the first injection of ions should occur before the shaded pink region. Therefore, there would be the second injection of ions in the shaded blue region, where the time variation of V_F is clearly ion-species–dependent, which will be examined in future publications.

On the second day V_F values of all ion species including both protons and heavy ions were between V_{SW} and V_A. All ions also kept their antisunward flow directions. In fact, even the reversal of the magnetic field, as seen in the shaded green region in Figure 8, did not change the similarity of flow directions between protons and heavy ions. The common flow direction of all ions in this far western solar longitude event is different from the opposite flow directions between protons and heavy ions observed in the well-connected or eastern solar longitude event described above. We discuss implications of our observations below.

For the 1998 November 14 event, pie plots of ion angular distributions are shown in Figure 9. We again see $\boldsymbol{V}_F$ of all ion species being antiparallel to $\boldsymbol{B}$ and $\boldsymbol{B}$ being nearly perpendicular to $\boldsymbol{V}_{SW}$.

4. DISCUSSIONS

4.1. *Bulk Flow Direction of Heavy Ions*

It is well known that the local magnetic field may be significantly different from the Parker spiral field line, especially in the front of IP shocks or both flanks of CMEs (e.g., Reames et al. 1996). Along the magnetic field the bulk flow direction of ions may not be antisunward, in particular during the eastern solar longitude events (e.g., Richardson et al. 1991; Richardson & Cane 1996). It was noted by Mason et al. (1989) and Tan & Mason (1993) that SEP events may have opposite flow directions. Therefore, it is interesting to see if in our selected SEP events various ion species have different flow directions.

The resolving power of the *Wind* LEMT sensor on ion species in the ion energy range of 2–10 MeV nucleon^{-1} provides us an opportunity to examine the possible difference of bulk flow

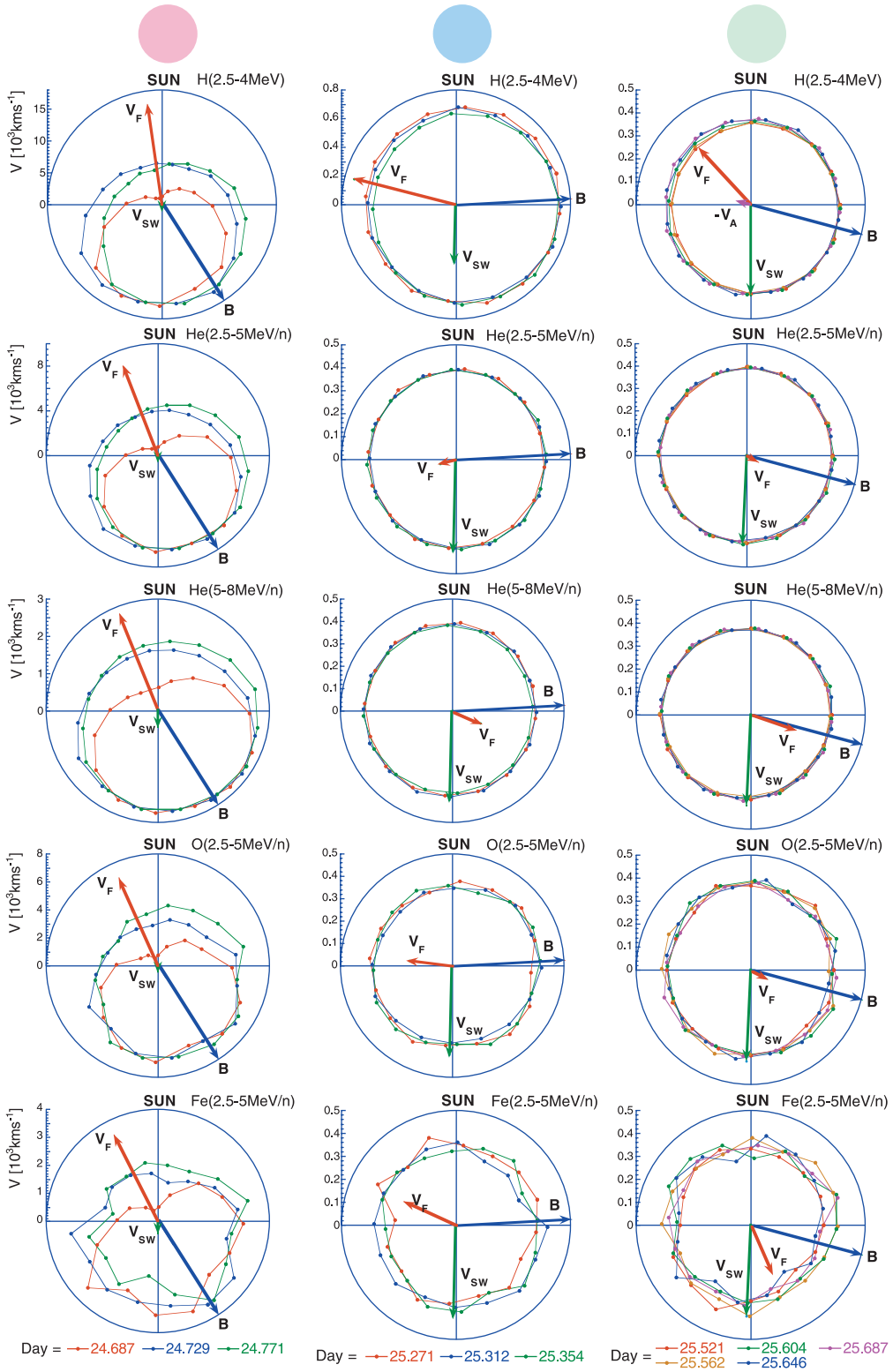

FIG. 7.—Same as Fig. 5, but for the 2001 September 24 SEP event.

directions among various ion species including H, He, O, and Fe ions. Our observations indicate that during the onset and rise phases, all ion species have common flow directions. In some events, during the plateau phase along the magnetic field direction, heavy ions may reverse their flow directions in sequence, i.e., faster ions reverse their directions earlier. Finally, in a shock-associated event, as the shock is approached, the flow directions of all heavy ions turn to be opposite to the proton flow.

Flow reversal of ions may be produced if there is a partially reflecting boundary beyond the observer (Bieber et al. 2002; Reames & Ng 2002). In order to explore such a possibility in the 2001 September 24 event, we exhibit the details of time variations of ϕ_F during the flow reversal interval in Figure 10, where ϕ_F of

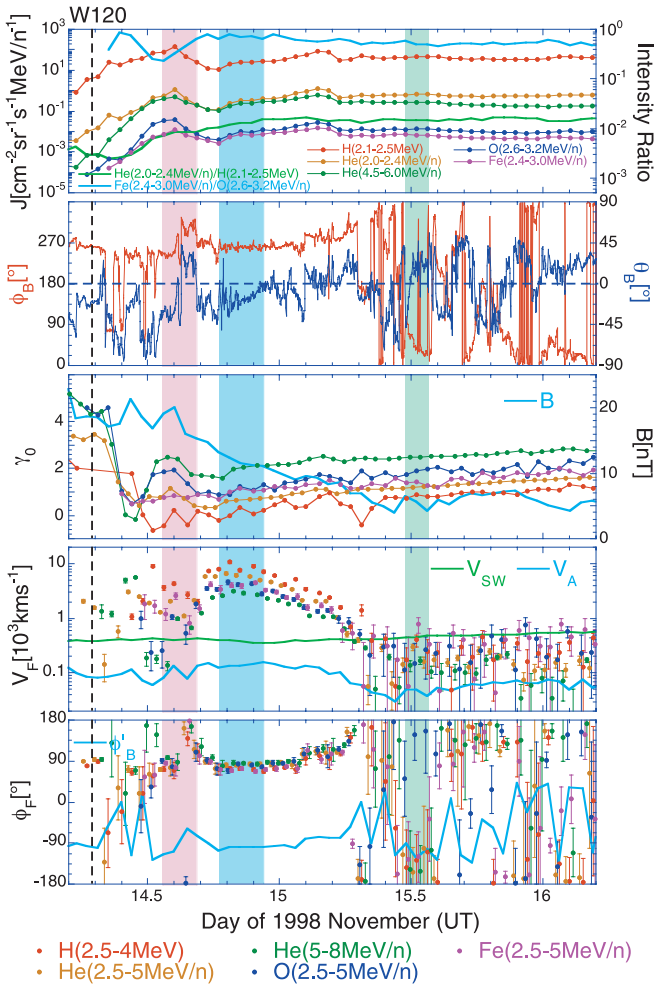

FIG. 8.—Same as Fig. 4, but for the 1998 November 14 SEP event.

heavy ions are compared with that of protons. Note that an error bar of ϕ_F with the magnitude similar to that of heavy ions should be also attached to proton data. It can be seen that higher speed He (5–8 MeV nucleon^{-1}) ions (with their mean kinetic energy $Tm \sim 6.1$ MeV nucleon^{-1}) first reversed their flow direction at $t_1 \sim 25.20$ days of 2001 September (UT). Then at $t_2 \sim 25.35$ days ($\sim$4 hr after t_1) lower speed He, O, and Fe ions at 2.5–5 MeV nucleon^{-1} with $Tm \sim 3.5$ MeV nucleon^{-1} reversed their flow directions simultaneously. Therefore, the flow-reversing time of heavy ions is ion velocity dependent (and not rigidity dependent).

A possible explanation as to why heavy ions reverse their flow directions in a velocity-dependent manner is that the *local* IP shock provides a significant number of freshly accelerated protons but fewer heavy ions. Temporal changes in the abundances of accelerated ions probably reflect changes in the seed population accelerated by the shock (e.g., Desai et al. 2003, 2004; Tylka et al. 2005). Thus, heavy ions would predominantly be accelerated nearer the Sun (e.g., the CME-driven IP shock in its earlier stage). Beyond 1 AU, there is evidence (Bieber et al. 2002; Reames & Ng 2002) indicating the possible existence of a reflecting outer boundary. In fact, magnetic field lines draped around the preceding CME can be viewed as a magnetic "mirror" (Tan et al. 1992b; Bieber et al. 2002), which plays the role of the suggested reflecting boundary. Thus, heavy ions may encounter the outer boundary and be reflected back to $\sim$1 AU, producing a directional reversal of their flows as observed on the *Wind* spacecraft. Higher speed ions would return to the spacecraft earlier because of their shorter traveling time, leading to an earlier reversal of their flow directions. However, see § 4.2 for the reason why proton flow reversal is not observed. In fact, the preceding CME with its speed $V_{\rm CME} = 633$ km s^{-1} is observable in the 2001 September 24 event (Gopalswamy et al. 2004). In contrast, the 1998 November 14 event, which shows no flow reversal, may be simply due to a lack of adequate reflecting boundary beyond 1 AU.

Assuming that the magnetic "mirror" in the flank of the preceding CME plays the role of the reflecting boundary of heavy ions, we can calculate the bounce period τ_b of a trapped particle between the point s_0 at 1 AU and the mirroring point s_m (Roederer 1970),

$$\tau_b = (2/v) \int_{s_0}^{s_m} ds\, [1 - B(s)/B_m]^{-1/2}, \qquad (11)$$

where the integral is carried out along the field line s and $B(s)$ is the magnetic field strength at the field line point s. It can be seen from equation (11) that $\tau_b \propto 1/v$, i.e., the flow reversing time of ions should be ion velocity–dependent, which is consistent with our observation in Figure 10.

Nevertheless, further numerical calculation of τ_b is not trivial in view of the following reasons.

1. The length of the real field line is unknown. Since the real field line will be draped around the preceding CME to form the bottleneck of field lines, which plays the role of magnetic mirroring, the real field line is significantly deflected from the nominal Parker spiral. It is difficult to estimate the length of the real field line because of unknown azimuthal width of the preceding CME.
2. In addition, the magnetic strength distribution along the real field line [i.e., $B(s)$] is unknown.
3. The ion scattering in the presence of a finite mean free path of ions would greatly complicate the scenario.

Therefore, from our observations, determining the characteristic parameters of the assumed outer reflecting boundary of ions is beyond the scope of this paper.

4.2. *Bulk Flow Direction of Protons*

The reason why upstream protons do not reverse their flow direction may be because the IP shock continues to accelerate a large number of protons but few heavy ions. The continuing addition of freshly accelerated protons dominates the reflected population, and so the proton flow remains away from the shock. Another possibility, which is not exclusive of that above, is that protons experience more scattering and trapping than the higher rigidity ions, and hence, fewer protons reach the boundary to be reflected back to 1 AU. That the local IP shock mainly provides freshly accelerated protons is consistent with Desai et al. (2003, 2004) who pointed out that ion acceleration in IP shocks has a systematic ion rigidity dependence with higher rigidity ions accelerated less efficiently than lower rigidity ions.

4.3. *Variation of Ion Bulk Flow Velocities during IP Shock Crossing*

For the 2001 September 24 event in which heavy ions also showed significant intensity enhancements when the IP shock was crossed as seen from Figure 6, there are *two* flow reversals of heavy ions. The first reversal occurred during day 25.2–25.4 of 2001 September as seen from Figures 6 and 10. After the reversal the flow direction of heavy ions changed from antiparallel to $\boldsymbol{B}$ to parallel to $\boldsymbol{B}$, while the proton flow was still antiparallel to $\boldsymbol{B}$, as

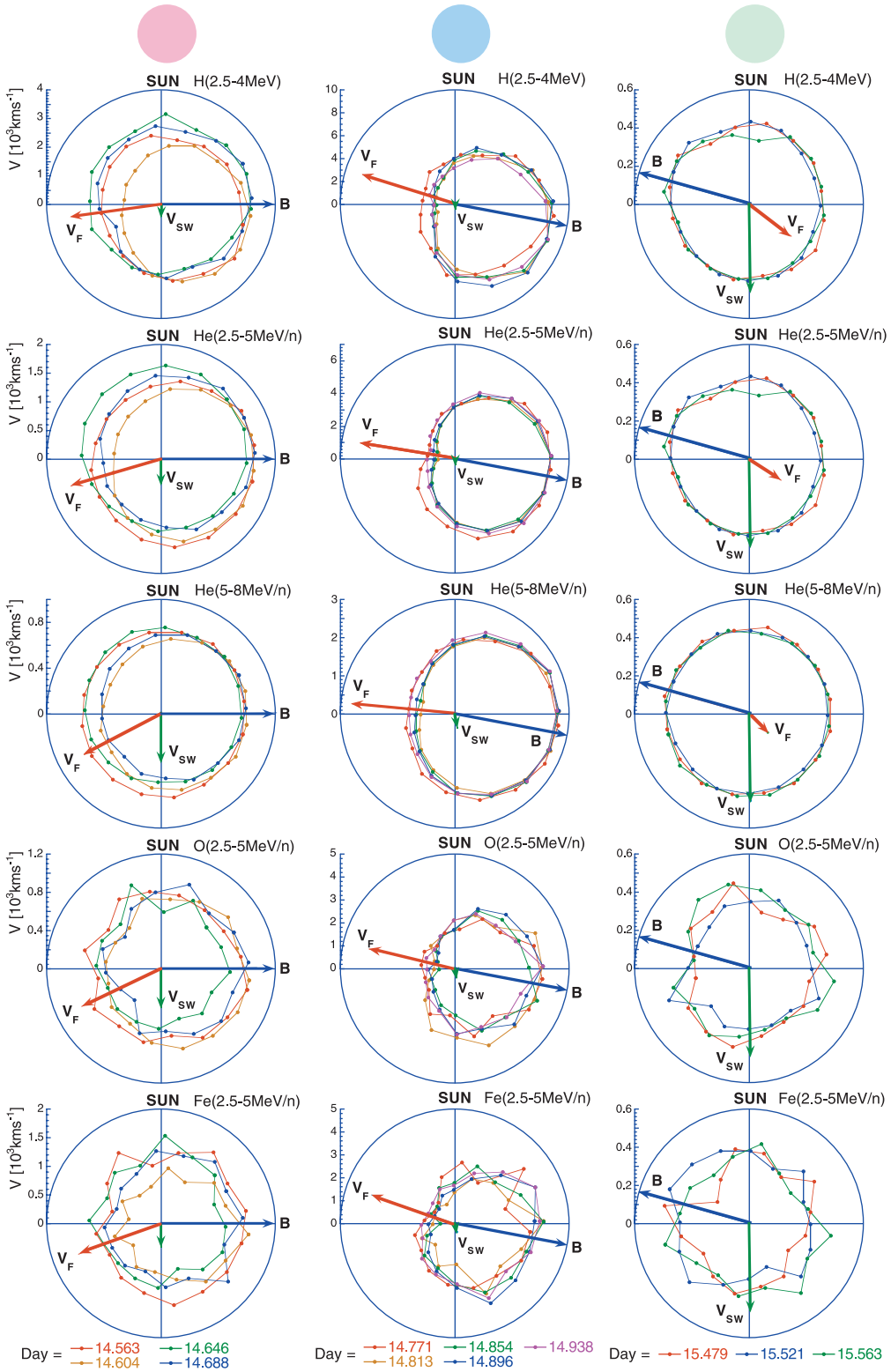

FIG. 9.—Same as Fig. 5, but for the 1998 November 14 SEP event.

seen from Figure 7. The second reversal occurred in the immediate upstream region of the IP shock as seen from Figure 11, where pie plots of ion angular distributions during the IP shock crossing period are shown. The time sequence is from bottom to top with 1 hr resolution in the figure, where the second flow reversal of heavy ions occurred during 17–19 hr of day 2001 September 25 (i.e., 2 hr before the IP shock passage; see the bottom two panels in Fig. 11), when the flow velocity of heavy ions changed from parallel to $\boldsymbol{B}$ back to antiparallel to $\boldsymbol{B}$.

The first flow reversal of heavy ions is due to the contribution of reflected ions as explained above. In fact, since there is a change in ion abundances at the shock with time (Desai et al. 2003, 2004), in the far upstream region the reflected heavy ions should have a higher intensity than newly accelerated heavy ions. The arrival of

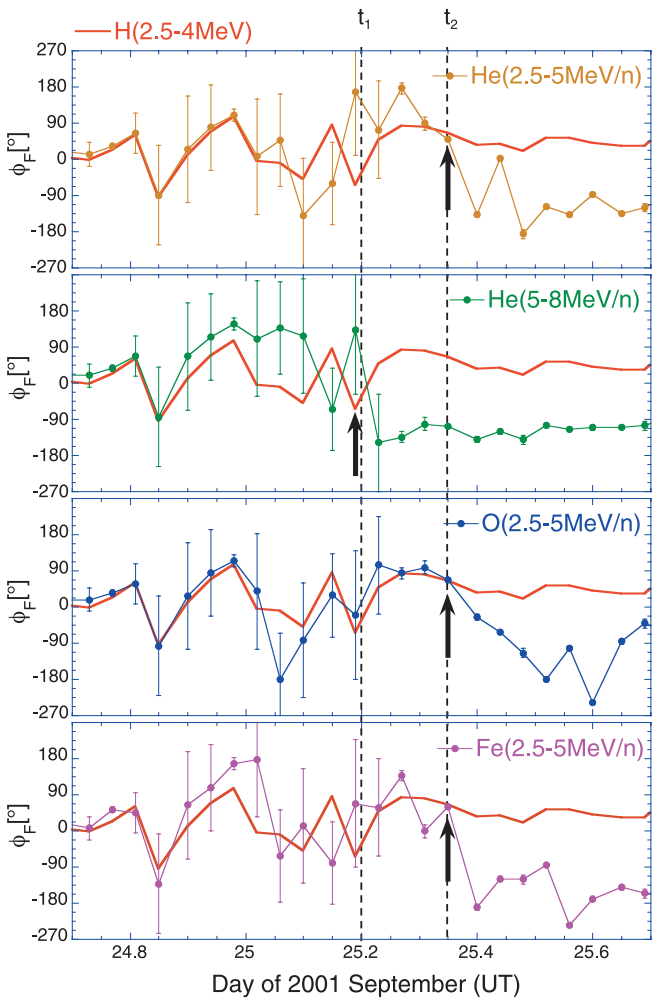

FIG. 10.—Comparisons of the azimuthal angle (ϕ_F) of heavy ions with that of protons in the 2001 September 24 SEP event.

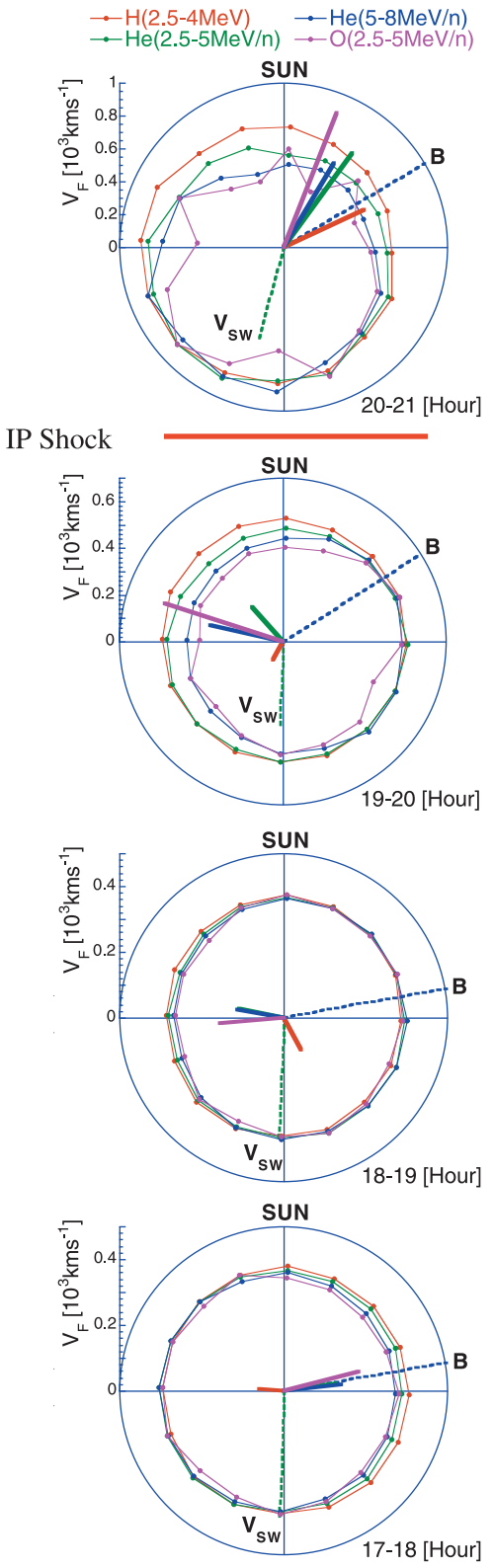

FIG. 11.—Angular distributions of different ion species during the IP shock crossing period in the 2001 September 24 SEP event.

reflected heavy ions would cause the reversal of heavy ion flows. On the other hand, immediately upstream of the IP shock the high intensity of heavy ions associated with the IP shock as shown by their intensity peaks would dominate the observed population of heavy ions, leading to their flows being outward of the shock (i.e., antiparallel to ***B***). Therefore, the observed double reversal of heavy ion flow is consistent with a limited upstream region in which the influence of heavy ions associated with the local IP shock is dominant.

In the bottom panel of Figure 11, we show a typical scenario widely observed in the plateau region; along ***B*** protons flow away from the shock, while heavy ions flow toward the shock. At the next hour (*third panel*) along ***B*** heavy ions flow away from the shock, while protons, which still flow away from the shock, have their antisunward flow direction. Furthermore, when the shock is approached (*second panel*) protons keep their antisunward flow direction, while the flows of heavy ions also turn sunward. Finally, downstream of the IP shock passage (*top panel*), nearly along ***B***, all ions show large sunward flows.

A drastic change of ion flow patterns occurs across the IP shock between the top and third panels in Figure 11. Along ***B*** the flows of protons and heavy ions change from outward upstream to inward downstream. Perpendicular to ***B***, proton and heavy ion flows are in opposite directions both upstream and downstream. The flows perpendicular to ***B*** are not consistent with pure solar-wind convection, indicating that transverse particle intensity gradient and/or perpendicular diffusion may play a role (Jokipii 1971; Zhang et al. 2003). Unfortunately, it is difficult to make any quantitative estimates in the absence of measurement of the spatial gradient of the SEPs.

TABLE 1
PROBABILITY THAT $-\boldsymbol{V}_A$ AT $V_w < 0$ DURING 2001 SEPTEMBER 25 12:00–16:00 (UT)

PARAMETER	VALUE FOR EACH ION SPECIES		
	He (2.5–5 MeV nucleon^{-1})	O (2.5–5 MeV nucleon^{-1})	Fe (2.5–5 MeV nucleon^{-1})
V_F (km s^{-1})	61 ± 31	82 ± 21	230 ± 140
ϕ_F (deg)	−120 ± 20	−130 ± 80	−160 ± 50
V_w^+ (km s^{-1})	87 ± 39	120 ± 60	60 ± 160
$P_r(V_w^+ < 0)$	0.012	0.023	0.35
V_w^- (km s^{-1})	−28 ± 39	0 ± 60	−50 ± 160
$P_r(V_w^- < 0)$	0.77	0.50	0.63
$P_r(-\boldsymbol{V}_A \mid V_w < 0)$	0.985	0.956	0.643

NOTES.—For this event $V_{SW} = 397 \pm 2$ km s^{-1}, $\phi_{SW} = 177.6^\circ \pm 0.4^\circ$, $\phi_B = 255^\circ \pm 4^\circ$, and $V_A = 58 \pm 3$ km s^{-1}.

4.4. *Propagating Direction of Proton-generated Alfvén Waves*

Upstream of IP shocks the scattering center of ions is driven by Alfvén waves mainly generated by protons (Lee 1983, 2005). In fact, a distribution of particles streaming along a field line is unstable and generates (or amplifies) Alfvén waves (Stix 1962; Melrose 1980). This process occurs independently of the nature of the source that accelerates the particles. The motion of waves is along $\boldsymbol{B}$ as Tsurutani et al. (1983) observed that the waves propagate within a cone of $\sim 15^\circ$ around $\boldsymbol{B}$.

While far upstream of the IP shock, our selected events have their magnetic field lines nearly perpendicular to the solar wind, they should not be called quasi-perpendicular shock events at 1 AU, because shock classification must be done in the immediate upstream region before shock passage, where Tylka et al. (2005) classified the events with $\theta_{Bn} > 70^\circ$ (where θ_{Bn} is the angle between the upstream magnetic field vector and the shock normal) as quasi-perpendicular and those with $\theta_{Bn} < 60^\circ$ as quasi-parallel. Among the three events examined above, however, the only one having the ESP peak surviving at 1 AU is the 2001 September 24 event, whose $\theta_{Bn} = 66^\circ \pm 18^\circ$, according to the shock list on the Web site of the University of New Hampshire Experimental Space Plasma Group.[4] The event is not a typical quasi-perpendicular shock event.

In fact, we have noted that quite a lot of shock events with significant ESP peaks at 1 AU are quasi-parallel. For example, the famous 2002 April 21 event examined in Tylka et al. (2005, 2006) has $\theta_{Bn} = 35^\circ \pm 8^\circ$, although their field line in the far upstream region is also nearly perpendicular to the solar wind. The occurrence of magnetic field lines nearly perpendicular to the solar wind is mainly due to the presence of the preceding CME. The magnetic field lines draped around the CME would change their configuration from the nominal Parker spiral to be nearly perpendicular to the solar wind.

Here we try to deduce a correct propagation direction of proton-generated Alfvén waves based on our suggested origin of heavy ions. During our selected periods when $\boldsymbol{V}_{SW}$ is nearly perpendicular to $\boldsymbol{B}$, the projection of $\boldsymbol{V}_{SW}$ along $\boldsymbol{B}$ is comparable to V_A. As a result, the direction of Alfvén wave propagation may significantly influence the parallel transport of heavy ions and the parallel component of their flow velocities. Hence, we may be able to determine the direction of Alfvén wave propagation based on the observation of $\boldsymbol{V}_F$.

We assume that heavy ions predominantly come from earlier acceleration near the Sun, while protons continue to be provided by the IP shock. With a partially reflecting boundary existing beyond 1 AU, the direction of diffusion of heavy ions would reverse, becoming opposite to that of protons. Since in the upstream region protons diffuse away from the shock, the diffusion of heavy ions should be toward the shock after their flow reversal.

Here we refer to the case shown in right panels of Figure 7, in which the angle between $\boldsymbol{B}$ and $\boldsymbol{V}_{SW}$ is $\leq 90^\circ$. Thus, the projection of $\boldsymbol{V}_{SW}$ along $\boldsymbol{B}$, $V_{SW,B}$ has the same sign as the projection of $\boldsymbol{V}_F$ along $\boldsymbol{B}$, $V_{F,B}$ for heavy ions. In addition, the Alfvén waves should propagate with velocity $-\boldsymbol{V}_A$ as denoted by the purple arrow in the top right (proton) panel, following the streaming direction of protons that excite the waves.

Based on the zero streaming condition in the rest frame, we have (Tan et al. 1989)

$$(v/3)(\partial f/\partial v)V_{wi} + \kappa_{ij}(\partial f/\partial x_j) = 0, \tag{12}$$

where x_i is the spatial coordinate, κ_{ij} is the diffusion tensor, and $\boldsymbol{V}_w$ is the ion scattering center velocity in the rest frame. The ion scattering center velocities in the solar-wind frame and spacecraft frame are $\boldsymbol{V}_{SC}$ and $\boldsymbol{V}_{SW} + \boldsymbol{V}_{SC}$, respectively. Since the velocity of the rest frame relative to the spacecraft frame is $\boldsymbol{V}_F$, the ion scattering center velocity in the rest frame is

$$\boldsymbol{V}_w = -\boldsymbol{V}_F + \boldsymbol{V}_{SW} + \boldsymbol{V}_{SC}. \tag{13}$$

In addition, because of $\gamma = -\partial \ln f/\partial \ln v$, equation (12) can be rewritten as

$$V_{wi} = 3\kappa_{ij}(\partial \ln f/\partial x_j)/\gamma. \tag{14}$$

To exclude from our consideration anisotropy contributions due to transverse spatial intensity gradient and/or perpendicular diffusion, we project V_{wi} along $\boldsymbol{B}$. By choosing the i-axis along $\boldsymbol{B}$ (i.e., by defining the coordinate axis $x_i = x_B$ along $\boldsymbol{B}$), from equation (14) we have the projection of V_{wi} along $\boldsymbol{B}$,

$$V_{wB} = 3\kappa_{\parallel}(\partial \ln f/\partial x_B)/\gamma, \tag{15}$$

where $\kappa_{\parallel}$ is the parallel diffusion coefficient. In addition, since $\boldsymbol{V}_F$ of protons is opposite to $\boldsymbol{B}$, $\boldsymbol{B}$ should be toward the shock. As described above, toward the shock there should be a negative gradient of heavy ions, we hence need $\partial \ln f/\partial x_B < 0$ for heavy ions. Under the condition that $\gamma > 0$, from equation (14) we finally need $V_{w,B} < 0$.

Assuming that ions are driven on Alfvén waves, we have $\boldsymbol{V}_{SC} = \pm \boldsymbol{V}_A$. By defining V_w^+ and V_w^- as the $V_{w,B}$ values obtained when $\boldsymbol{V}_{SC}$ are equal to $\boldsymbol{V}_A$ and $-\boldsymbol{V}_A$, respectively, from equations (13)–(15) we have along $\boldsymbol{B}$

$$V_w^{\pm} = -V_{F,B} + V_{SW,B} \pm V_A < 0. \tag{16}$$

[4] See http://www.ssg.sr.unh.edu.

The values of V_w^+ and V_w^- can be calculated by using the bootstrap method (Efron & Tibshirani 1991). Our calculation results are listed in Table 1, where $P_r(V_w^+ < 0)$ and $P_r(V_w^- < 0)$ are the probabilities that $V_w^+ < 0$ and $V_w^- < 0$, respectively. The details of probability calculations are given in the Appendix.

From Table 1 it can be seen that we have a high probability of identifying that $\boldsymbol{V}_{\rm SC} = -\boldsymbol{V}_{\rm A}$, i.e., $\boldsymbol{V}_{\rm A}$ should be antiparallel to $\boldsymbol{B}$, indicating that the direction of $\boldsymbol{V}_{\rm A}$ follows the flow direction of protons away from the shock (Fig. 7, *top right*). In fact, from data of all three heavy ion species, we obtain the probability that $\boldsymbol{V}_{\rm SC} = \boldsymbol{V}_{\rm A}$ (i.e., $\boldsymbol{V}_{\rm A}$ is parallel to $\boldsymbol{B}$) is less than 2.4×10^{-4}. Our result is consistent with Kennel et al. (1986), who found that upstream of IP shocks the observed waves flow away from the IP shock. It should be emphasized that if the diffusive motion of heavy ions is assumed to be the same as protons, the deduced $\boldsymbol{V}_{\rm A}$ would have the direction opposite to streaming protons. Therefore, our suggested origin of heavy ions can provide a correct identification of propagating direction of Alfvén waves.

5. SUMMARY

The main results obtained from this work can be summarized as follows.

1. The bulk flow velocities of H, He, O, and Fe ions in the MeV nucleon^{-1} energy range are deduced for three "gradual" SEP events having different solar longitudes.

2. During the onset phase both protons and heavy ions have common flow directions. However, in two of the three events studied, during the "plateau" phase, the flow directions of heavy ions reverse in sequence, i.e., faster ions reverse their directions earlier, suggesting the presence of a reflecting boundary beyond 1 AU. Finally, when the IP shock is approached the flows of all heavy ions are opposite to the proton flow until we are very near the shock, where the component of the flow along $\boldsymbol{B}$ for all species is away from the shock, both upstream and downstream.

3. Evidence suggests that the local IP shock provides freshly accelerated protons, but a diminishing number of heavy ions to the upstream region. Heavy ions are more strongly accelerated nearer the Sun and propagate through the heliosphere. Beyond 1 AU, the particles may be reflected from the outer boundary of a SEP confinement volume and return to 1 AU in significant numbers to reverse the flow.

4. When the upstream magnetic field is nearly perpendicular to the solar-wind velocity, the favorable geometric condition allows us to determine the propagating direction of proton-generated Alfvén waves based on the flow velocity data of heavy ions.

We thank K. Ogilvie for the use of *Wind* plasma data from the Solar Wind Experiment (SWE), R. Lepping for the use of *Wind* IMF data from the Magnetic Field Experiment (MFE), and B. McGuire for the use of *IMP 8* proton data. We thank K. Ogilvie and X. Shao for many helpful discussions. We also thank the anonymous reviewer for his/her valuable comments. C. K. N. is supported under NASA proposals LWS04-0000-0076 and SHP04-0016-0024.

APPENDIX

PROBABILITY CALCULATIONS

As listed in Table 1, $P_r(V_w^+ < 0)$ and $P_r(V_w^- < 0)$ are the probabilities that $V_w^+ < 0$ and $V_w^- < 0$, respectively. Since

$$P_r(V_w^+ < 0) = P_r(V_w < 0 | \boldsymbol{V}_{\rm A}) = P_r(V_w < 0; \boldsymbol{V}_{\rm A})/P_r(\boldsymbol{V}_{\rm A}), \tag{A1}$$

and

$$P_r(V_w^- < 0) = P_r(V_w < 0 | -\boldsymbol{V}_{\rm A}) = P_r(V_w < 0; -\boldsymbol{V}_{\rm A})/P_r(-\boldsymbol{V}_{\rm A}), \tag{A2}$$

where $P_r(A|B)$ denotes the conditional probability that event A occurs under the presence of event B. The probability of $-\boldsymbol{V}_{\rm A}$ at the observed $V_w < 0$ is

$$P_r(-\boldsymbol{V}_{\rm A} | V_w < 0) = P_r(-\boldsymbol{V}_{\rm A}; V_w < 0)/P_r(V_w < 0). \tag{A3}$$

Since

$$P_r(V_w < 0) = P_r(V_w < 0; -\boldsymbol{V}_{\rm A}) + P_r(V_w < 0; \boldsymbol{V}_{\rm A}), \tag{A4}$$

we further have

$$\begin{aligned} P_r(-\boldsymbol{V}_{\rm A} | V_w < 0) &= P_r(-\boldsymbol{V}_{\rm A}; V_w < 0)/[P_r(V_w < 0; -\boldsymbol{V}_{\rm A}) + P_r(V_w < 0; \boldsymbol{V}_{\rm A})] \\ &= P_r(V_w^- < 0) P_r(-\boldsymbol{V}_{\rm A})/\left[P_r(V_w^- < 0) P_r(-\boldsymbol{V}_{\rm A}) + (P_r(V_w^+ < 0) P_r(\boldsymbol{V}_{\rm A})\right] = P_r(V_w^- < 0)/\left[P_r(V_w^- < 0) + P_r(V_w^+ < 0)\right], \end{aligned} \tag{A5}$$

where we assume that $P_r(-\boldsymbol{V}_{\rm A})/P_r(\boldsymbol{V}_{\rm A}) = 1$, i.e., without the limitation of V_w, $\pm\boldsymbol{V}_{\rm A}$ have equal probabilities. Calculation results based on equation (A5) are listed in Table 1.

REFERENCES

Bieber, J. W., et al. 2002, ApJ, 567, 622
Desai, M. I., Mason, G. M., Wiedenbeck, M. E., Mazur, J. E., Gold, R. E., Krimigis, S. M., Smith, C. W., & Skoug, R. M. 2003, ApJ, 588, 1149
———. 2004, ApJ, 611, 1156
Dwyer, J. R., Mason, G. M., Mazur, J. E., Jokipii, J. R., von Rosenvinge, T. T., & Lepping, R. P. 1997, ApJ, 490, L115
Efron, B., & Tibshirani, R. 1991, Science, 253, 390
Forman, M. A. 1968, J. Geophys. Res., 73, 5783
———. 1970, Planet. Space Sci., 18, 25
Forman, M. A., & Gleeson, L. J. 1975, Ap&SS, 32, 77
Gleeson, L. J. & Axford, W. I. 1968, A&SS, 2, 431
Gleeson, L. J., & Webb, G. M. 1980, Fund. Cosmic Phys. 6, 187

Gloeckler, G., Scholer, M., Ipavich, F. M., Scholer, M., Hovestadt, D., & Klecker, B. 1984, Geophys. Rev. Lett., 11, 603
Gopalswamy, N., et al. 2004, J. Geopys. Res., 109, A12105
Gordon, B. E., Lee, M. A., Möbius, E., & Trattner, K. J. 1999, J. Geophys. Res., 104, 28263
Ipavich, F. M. 1974, Geophys. Rev. Lett., 1, 149
Jokipii, J. R. 1971, Rev. Geophys. 9, 27
Kahler, S. W. 2005, ApJ, 628, 1014
Kennel, C. F., Coroniti, F. V., Scarf, F. L., Livesey, W. A., Russell, C. T., & Smith, E. J. 1986, J. Geophys. Res., 91, 11917
Lario, D., et al. 2000a, J. Geophys. Res., 105, 18235
———. 2000b, J. Geophys. Res., 105, 18251
Lee, M. A. 1983, J. Geophys. Res. 88, 6109
———. 2005, ApJS, 158, 38
Lesky, R. A., et al. 2001, in Proc. 27th Int. Cosmic Ray Conf. (Hamburg), 3269
Mason, G. M., Ng, C. K., Klecker, B., & Green, G. 1989, ApJ, 339, 529
McCraken, K. G., & Ness, N. F. 1966, J. Geophys. Res., 71, 3315
McCraken, K. G., Rao, K. G., Bukata, U. R., & Keath, E. P. 1971, Sol. Phys., 18, 100
Melrose, D. B. 1980, Plasma Astrophysics, Vol. 1 (New York: Gordon & Breach)
Ng, C. K. 1986, Ap&SS, 126, 313
———. 1987, Sol. Phys., 114, 165
Ng, C. K., & Gleeson, L. J. 1971, Sol. Phys., 20, 166
Ng, C. K., Reames, D. V., & Tylka, A. J. 2003, ApJ, 591, 461
Ng, C. K., & Wong, K. Y. 1979, in Proc. 16th Int. Cosmic Ray Conf. (Kyoto), 5, 252
Reames, D. V. 1999, Space Sci. Rev., 90, 413
———. 2000a, ApJ, 540, L111
———. 2000b, in AIP Conf. Proc. 528, Acceleration and Transport of Energetic Particles Observed in the Heliosphere, ed. R. A. Mewaldt et al. (Melville: AIP), 79
Reames, D. V., Barbier, L. M., & Ng, C. K. 1996, ApJ, 466, 473
Reames, D. V., & Ng, C. K. 2002, ApJ, 577, L59
Reames, D. V., Ng, C. K., & Berdichevsky, D. 2001, ApJ, 550, 1064
Richardson, I. G., & Cane, H. V. 1996, J. Geophys. Res., 101, 27521
Richardson, I. G., Cane, H. V., & von Rosenvinge, T. T. 1991, J. Geophys. Res., 96, 7853
Roederer, J. G. 1970, Dynamics of Geomagnetically Trapped Radiation (New York: Springer)
Roelof, E. C. 1969, in Lectures in High Energy Astrophysics, ed. H. Ögelman & J. R. Wayland (NASA SP-199; Washington: NASA), 111
Sanderson, T. R., Marsden, R. G., Tranquille, C., Dalla, S., Forsyth, R. J., Gosling, J. T., & McKibben, R. B. 2003, Geophys. Res. Lett., 30, 8036
Sanderson, T. R., Reinhard, R., van Ness, P., Wenzel, K.-P., Smith, E. J., & Tsurutani, B. T. 1985, J. Geophys. Res., 90, 3973
Stix, T. H. 1962, The Theory of Plasma Waves (New York: McGraw-Hill)
Tan, L. C., & Mason, G. M. 1993, ApJ, 409, L29
Tan, L. C., Mason, G. M., Gloeckler, G., & Ipavich, F. M. 1988, J. Geophys. Res., 93, 7225
———. 1989, J. Geophys. Res., 94, 6552
Tan, L. C., Mason, G. M., Gloeckler, G., & Klecker, B. 1992a, J. Geophys. Res., 97, 179
Tan, L. C., Mason, G. M., Lee, M. A., Klecker, B., & Ipavich, F. M. 1992b, J. Geophys. Res., 97, 1597
Tsurutani, B. T., Smith, E. J., & Jones, D. E. 1983, J. Geophys. Res., 88, 5645
Tylka, A. J., Cohen, C. M. S., Dietrich, W. F., Lee, M. A., Maclennan, C. G., Mewaldt, R. A., Ng, C. K., & Reames, D. V. 2005, ApJ, 625, 474
———. 2006, ApJS, 164, 536
von Rosenvinge, T. T., et al. 1995, Space Sci. Rev., 71, 155
Zhang, M., et al. 2003, J. Geophys. Res., 108, 1154